Ballistic thermal conductance of electrons in graphene ribbons

Eiji Watanabe, Sho Yamaguchi, Jun Nakamura,* and Akiko Natori†
Department of Electronic-Engineering, The University of Electro-Communications, 1-5-1 Chofugaoka, Chofu, Tokyo 182-8585, Japan
(Received 11 March 2009; revised manuscript received 16 July 2009; published 4 August 2009)

We investigate the ballistic thermal conductance of electrons in gated graphene ribbons with width above 20 nm and clarify both the temperature and the Fermi-level dependences. In the intrinsic graphene ribbons, the normalized thermal conductance by the quantum conductance, κ_0, increases monotonically with temperature. In the gated graphene ribbons, the normalized thermal conductance increases steplikely as the Fermi level increases but it has nonmonotonic temperature dependence when the Fermi level is a little larger than the bottom of the subband. The value of the step height changes from $4\kappa_0$ to $2\kappa_0$ with increasing temperature. The ballistic electron thermal conductance per unit width of graphene ribbons is smaller than those of corresponding single-walled nanotubes and a graphene sheet and it approaches at 100 K that of a graphene sheet above the ribbon width of about 80 and 50 nm for zigzag ribbons and armchair ribbons, respectively.

DOI: 10.1103/PhysRevB.80.085404 PACS number(s): 68.65.−k, 44.10.+i, 65.80.+n, 81.05.Uw

I. INTRODUCTION

The exceptional electronic transport properties of low-dimensional graphitic structures have been extensively demonstrated in carbon nanotubes.[1] With respect to the electronic-transport properties, ballistic transport has been observed up to room temperature in carbon nanotubes. As for the thermal transport, thermal conductivity of single-walled carbon nanotubes has been measured[2] and the observed T-linear temperature dependence below 50 K has been explained well by the ballistic thermal transport.[3] In the ballistic limit, the thermal conductance of one-dimensional (1D) system is quantized by the quantum conductance, $\kappa_0 = \pi^2 k_B^2 T/3h$ and the metallic single-walled carbon nanotubes have a thermal conductance of $8\kappa_0$ at low temperatures. Here, $4\kappa_0$ is contribution of four acoustic phonon modes and the remaining $4\kappa_0$ is contribution of two electronic bands which cross the Fermi level.

On the other hand, a graphene, a single atomic layer of graphite, which is two-dimensional form of carbon, is found to exhibit high crystal quality and to have ballistic electronic transport at room temperature. Graphene-based electronics has attracted much attention due to high carrier mobility in the bulk graphene. Recently, graphene ribbons have also been interested since the electronic structure can be controlled by both the edge shape and the ribbon width, just as carbon nanotubes. Very recently, chemically derived ultrasmooth graphene nanoribbons (GNR) with width below 10 nm has been produced.[4] Electrical-transport experiments showed that all of the sub-ten-nanometer GNRs were semiconductors and afforded graphene-field-effect transistors (FET) with on-off ratios of about 10^7 at room temperature. The performance of GNR-FET operation at a room temperature has been analyzed for the device with the width and length of 2 and 236 nm, respectively.[5] The ratio of the ballistic current was analyzed to be about 21% and 4.5%, respectively, at $V_{ds}=1$ V and $V_{ds}<0.1$ V. The small ballisticity at low drain bias is thought to be caused by edge elastic scattering. Extensive studies have been tried to produce straight edge narrow GNRs and recently GNRs have been produced also from carbon nanotubes by unzipping process.[6,7]

The recent demonstration of field effect in a graphene and GNRs has opened a new research venue. The electronic structure of gated graphene and graphene ribbons has been studied in the Hartree approximation on the basis of tight-binding model.[8] By applying the gate bias, carriers are injected and the Fermi level can be shifted relative to that of the intrinsic graphene or graphene ribbons. The change of the band structure caused by the electron-electron Coulomb interaction is shown to be not so large for the gated graphene ribbons. Performance limits has also been studied for GNR-FETs with a constriction, based on the Landauer formula in the tight-binding model.[9] Simulations were also performed to assess the effects of static disorder on the conductance of metallic armchair- and zigzag-edge GNRs in the tight-binding model.[10] GNRs were found to have outstanding ballistic transport properties in the presence of a substrate-induced disorder. However, only the zigzag-edge GNRs retain the ballisticity in the presence of edge disorder.

The electronic structure of graphene ribbons was studied for the first time in the tight-binding approximation by Fujita's group[11,12] and the ribbons are classified into two typical types, a zigzag ribbon and an armchair ribbon, by their edge shapes. The zigzag ribbons with zigzag edges are metallic and the Fermi energy is located at the flat band of which wave function is localized in the vicinity of the zigzag edges. The armchair ribbons, on the other hand, are metallic or semiconducting depending on the ribbon width. Recently, the energy band gap of graphene nanoribbons has been measured actually and larger energy gaps opening is shown for narrowing ribbons below 20 nm while the expected directional dependence could not been confirmed.[13] The width dependence of the band gaps of GNRs was calculated for ribbon width below 10 nm, based on a first-principles approach.[14] Both armcahir and zigzag ribbons are shown to have band gaps, contrary to the tight-binding calculations. The origin of the energy gaps for GNRs with armchair edges arises from both the quantum confinement and the relaxation of edges and that for GNRs with zigzag edges does from a staggered sublattice potential on the hexagonal lattice due to the edge magnetization.

In our previous paper, we studied the Fermi-level dependence of the ballistic thermal conductance for the gated graphene sheets[15] and showed that the electronic contribution can be more dominant than phonon contribution in low temperatures if the Fermi level is sufficiently large. Recently, the thermal conductance of a graphene sheet has been measured actually at a room temperature and it exhibits a value close to the ballistic thermal conductance.[16] The ballistic thermal conductance of a graphene, on the other hand, is shown to give the lower limit of the ballistic thermal conductance per unit circumference length of carbon nanotubes.[17]

Our purpose is to calculate the ballistic thermal conductance of electrons in gated graphene ribbons in a wide range of ribbon width and to clarify the dependence on both the temperature and the Fermi level. As for the phonon contribution to the ballistic thermal conductance of GNRs, κ_{ph} has a value of $3\kappa_0$ at low temperatures irrespective of both the ribbon width and the edge shape, corresponding to three acoustic phonon modes.[18] The normalized thermal conductance by κ_0 begins to increase with temperature at $T=4$ K for a zigzag ribbon of $N_z=8$ and for an armchair ribbon of $N_a=11$.[18]

II. FORMULATION

First, we formulate the ballistic thermal conductance of electrons in 1D system. The ballistic thermal current of the 1D electron system formed between a hot heat bath and a cold heat bath arranged in the x direction is described as the Landauer heat flux as follows:

$$\dot{Q}_{\text{el}} = 2\sum_m \int_{v_m>0} \frac{dk}{2\pi}[\varepsilon_m(k)-\mu]v_m(k)\{f[\varepsilon_m(k),\mu,T_{\text{hot}}] - f[\varepsilon_m(k),\mu,T_{\text{cold}}]\}, \tag{1}$$

where $\varepsilon_m(k)$ represents the 1D electron-energy dispersion relation of the mth band along the ribbon axis, $v_m(k)=\frac{\partial\varepsilon_m(k)}{\hbar\partial k}$ is the electron group velocity and $f[\varepsilon_m(k),\mu,T]$ is the Fermi-distribution function with the Fermi level μ at a temperature T. Here, the transmission coefficient for each electron state is assumed to be unity. Changing the integration variable in Eq. (1) from k to $x_m=[\varepsilon_m(k)-\mu]/k_BT$ and assuming the linear dependence of $\dot{Q}_{\text{el}}$ on $\Delta T=T_{\text{hot}}-T_{\text{cold}}$, the thermal conductance of electrons, $\kappa_{\text{el}}=\dot{Q}_{\text{el}}/\Delta T$, can be written as

$$\kappa_{\text{el}} = \sum_m \frac{2k_B^2T}{h}\int_{v_m>0} x_m^2\frac{\exp(x_m)}{[\exp(x_m)+1]^2}dx_m. \tag{2}$$

Here, it should be mentioned that the indefinite integral of Eq. (2) can be obtained analytically as follows for $x>0$:

$$\int^x x'^2\frac{\exp(x')}{[\exp(x')+1]^2}dx' = -\frac{x^2\exp(-x)}{[1+\exp(-x)]} - 2x\log[1+\exp(-x)] + \sum_{n=1}^{\infty}(-1)^n\frac{2\exp(-nx)}{n^2}. \tag{3}$$

The similar equation can be derived for $x<0$. The contribution of single energy band which crosses the Fermi level with positive group velocity has $2\kappa_0$ at $T=0$ where $\kappa_0=\pi^2k_B^2T/3h$ is the thermal quantum conductance, since

$$\sum_{n=1}^{\infty}\frac{(-1)^{n-1}}{n^2}=\frac{\pi^2}{12}. \tag{4}$$

Here a factor 2 in $2\kappa_0$ is attributed to the spin degeneracy. We consider two typical types of graphene ribbons, a zigzag ribbon and an armchair ribbon, as shown in Fig. 1. In the following numerical calculation of κ_{el}, the dispersion relations of $\varepsilon_m(\boldsymbol{k})$ are calculated in the tight-binding approximation to obtain the band structure of graphene ribbons in a wide range of widths. We consider only the π band since the σ band is distant from the Fermi level. We use parameters,[1] the nearest-neighbor transfer integral, $t=-3.033$ eV, the overlap integral, $S=0.129$, and the lattice constant of a graphene sheet, $a=0.246$ nm. Typical dispersion relations are shown in Fig. 2 for both a zigzag ribbon and a metallic armchair ribbon. A zigzag ribbon has a flat band with two-

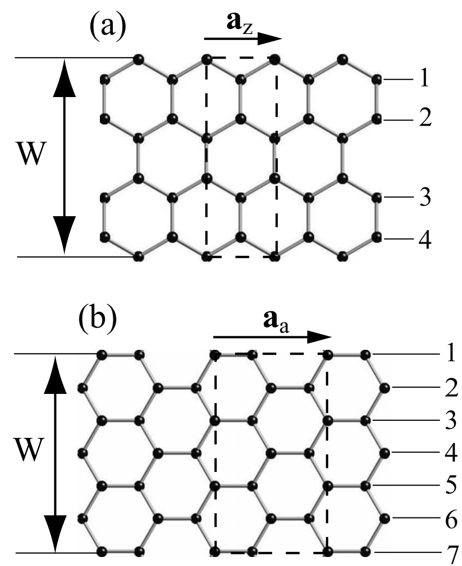

FIG. 1. Schematic figures of (a) a zigzag ribbon with a width of $N_z=4$ and (b) an armchair ribbon with $N_a=7$.

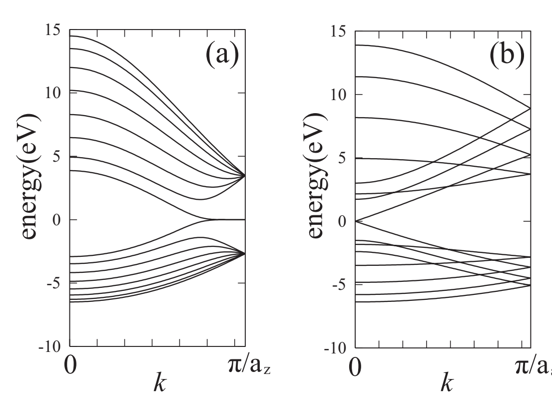

FIG. 2. Energy dispersion relations in the tight-binding model of (a) a zigzag ribbon with a width of $N_z=8$ and (b) an armchair ribbon with $N_a=8$.

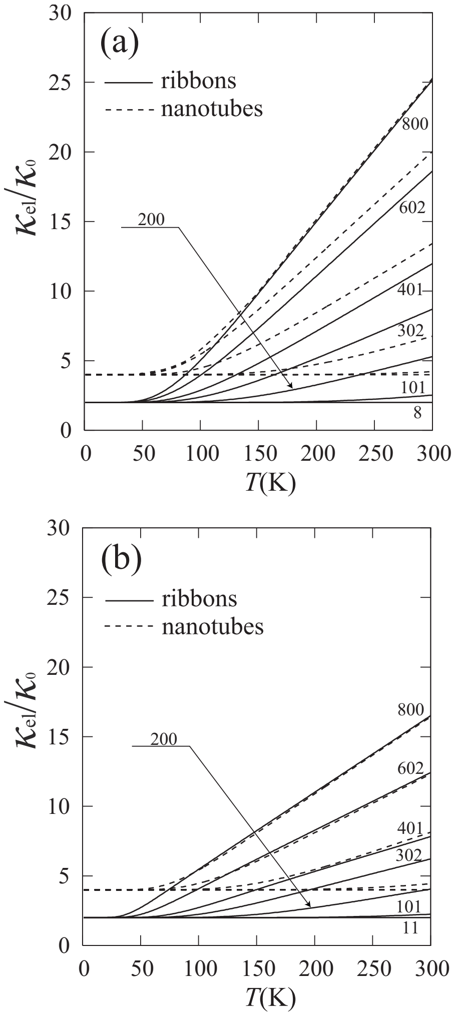

FIG. 3. Electron-derived thermal conductance κ_{el} in the tight-binding model of (a) zigzag ribbons at $N_z = 8, 101, 200, 302, 401, 602, 800$ and (b) armchair ribbons at $N_a = 11, 101, 200, 302, 401, 602, 800$ as a function of temperature. κ_{el} for (400,400), (300,300), (200,200),(100,100), (50,50), and (4,4) armchair nanotubes are also plotted by broken lines in (a) and those for (399,0), (300,0), (201,0), (99,0), (51,0), and (6,0) zigzag nanotubes are plotted by broken lines in (b). No temperature dependence is noticed for two narrowest zigzag nanotubes in (b).

fold degeneracy at the intrinsic Fermi level which is taken to be zero. An armchair ribbon, on the other hand, is metallic for a ribbon width of $N_a = 3M-1$, where M is an integer and otherwise semiconducting. In the metallic armchair ribbons, two bands crosses the intrinsic Fermi level. First-principles calculations of H-terminated zigzag graphene ribbons exhibit the similar electronic structure for π bands.[19,20] However, recent first-principles calculations show opening of the band gap for sub-ten-nm graphene ribbons[14,21–23] and we discuss the effect on the ballistic thermal conductance in the Sec. IV.

III. NUMERICAL RESULTS

First, we present in Fig. 3 the normalized ballistic thermal conductance by the quantum conductance, κ_0, in the intrinsic graphene ribbons as a function of temperature for both zigzag ribbons and armchair ribbons. Only the states at the Fermi level contribute at very low temperatures and hence the ballistic thermal conductance below about 50 K is determined mainly by two bands which touch the intrinsic Fermi level and one band which crosses the intrinsic Fermi level with positive group velocity, respectively, for zigzag and armchair ribbons in the tight-binding model. As temperature increases, both the higher and the lower bands than the Fermi level begin to contribute and the normalized thermal conductance increases monotonically with temperature.

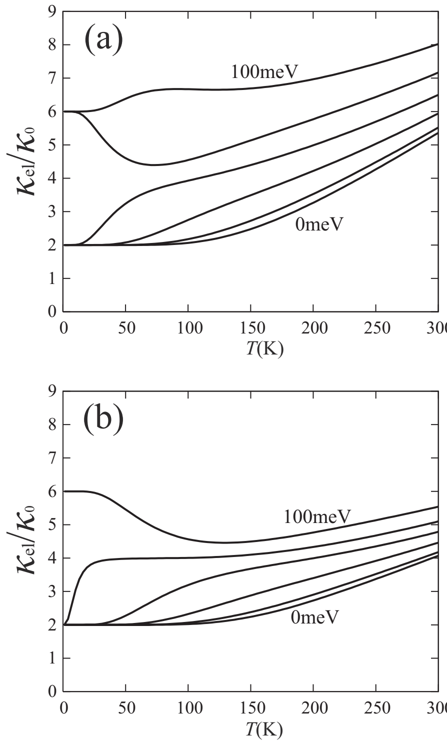

FIG. 4. Electron-derived thermal conductance κ_{el} of (a) a zigzag ribbon with $N_z=200$ and (b) an armchair ribbon with $N_a=200$ at $\mu=0, 20, 40, 60, 80, 100$ meV as a function of temperature.

Second, we present in Fig. 4 the normalized ballistic thermal conductance of electrons in the gated graphene ribbons for both a zigzag ribbon with $N_z=200$ and an armchair ribbon with $N_a=200$, as a function of temperature. It is seen that the normalized thermal conductance at $T=0$ increases by $4\kappa_0$ as the Fermi level crosses the bottom of the excited bands. When the Fermi level is just above the bottom of the excited band, the electron contribution just below the Fermi level disappears with increasing temperature and hence its temperature dependence exhibits nonmonotonic behavior with a valley. In the temperature dependence of the thermal conductance itself instead of the normalized conductance by κ_0, κ_{el} increases monotonically with temperature and has a point of inflection since κ_0 is proportional to T. In Figs. 5 and 6, we plot the normalized thermal conductance as a function of the Fermi level, for zigzag ribbons and armchair ribbons, respectively. A staircase with a height of $4\kappa_0$ at $T=1$ K changes to a staircase with a height of $2\kappa_0$ at $T=100$ K for both the zigzag ribbons and armchair ribbons. The step height of $4\kappa_0$ at $T=1$ K for zigzag ribbons is at-

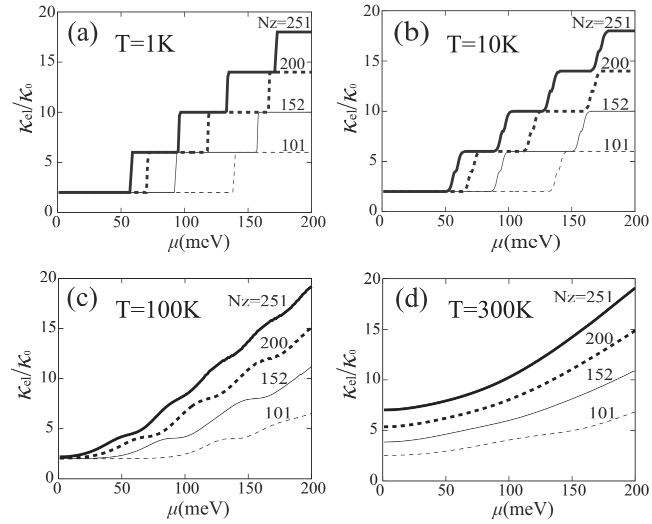

FIG. 5. Electron-derived thermal conductance κ_{el} of zigzag ribbons with $N_z=101,152,200,251$, as a function of the Fermi level, μ, at (a) $T=1$ K, (b)$T=10$ K, (c)$T=100$ K, and (d) $T=300$ K.

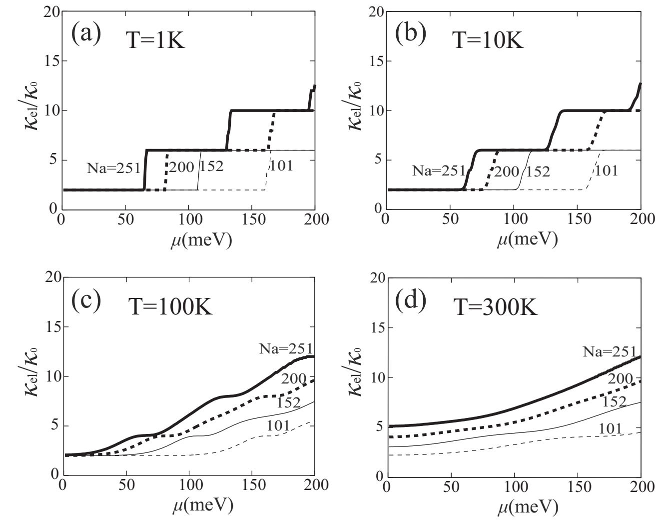

FIG. 6. Electron-derived thermal conductance κ_{el} of armchair ribbons with $N_a=101,152,200,251$, as a function of the Fermi level, μ, at (a) $T=1$ K, (b) $T=10$ K, (c) $T=100$ K and (d) $T=300$ K.

tributed to two minima at $\pm k_0$ for each excited subband and that for armchair ribbons is attributed to neary twofold-degenerate minima at $k=0$ for each excited subband. The change in the step height to $2\kappa_0$ at 100 K is caused by the valley structure in Fig. 4, i.e., negligible occupation probability of electrons near the bottom of the excited subbands just below the Fermi level. On the other hand for negative values of the Fermi level, μ, i.e., for hole injection, the same behavior can be obtained. This electron-hole symmetry is attributed to the k-linear dispersion relation in the vicinity of the intrinsic Fermi level located at the Dirac point in a graphene sheet.

IV. DISCUSSION AND CONCLUSION

First, we remark on the relation between the ballistic thermal conductance of electrons in graphene ribbons and single-walled carbon nanotubes,[1] in the tight-binding model. The (n,n) armchair nanotubes has $4n$ π bands and can be formed by rolling along the ribbon axis the zigzag ribbons with a width of $N_z=2\ n$. On the other hand, $(n,0)$ zigzag nanotube has $4n$ π bands and can be formed by rolling along the ribbon axis the armchair ribbons with a width of $N_a=2\ n$. Indeed, armchair nanotubes are always metallic as zigzag ribbons and zigzag nanotubes are metallic when n is a multiple of 3 and otherwise semiconducting as armchair ribbons. However, two bands crosses the Fermi level for metallic nanotubes and the electronic thermal conductance has $4\kappa_0$ at low temperatures instead of $2\kappa_0$ of metallic graphene ribbons in the tight-binding model. The thermal conductance of electrons in armchair nanotubes and zigzag nanotubes are also plotted in Figs. 3(a) and 3(b), respectively. The single-walled (n,n) or $(n,0)$ carbon nanotubes with $n>200$ in Fig. 3 have approximately similar magnitudes to the corresponding nanoribbons at 100 K in the tight-binding model. This means that the edge effect of ribbons almost diminishes at 100 K for wide ribbons with $N_z>400$ or $N_a>400$.

Second, we comment on the ballistic thermal conductance per unit width of intrinsic graphene ribbons. In the tight-binding model, the thermal conductance per unit width approaches that of a graphene sheet at 100 K above $W_z=80$ nm ($N_z=376$) and $W_a=50$ nm ($N_a=408$) for zigzag ribbons and armcahir ribbons, respectively. In contrast to the tight-binding model, the first-principles calculation predicts opening of the energy gap for narrow sub-ten-nanometer ribbons.[14] At the ribbon widths of $W_z=80$ nm and $W_a=50$ nm, the extrapolated energy gaps from those of the sub-ten-nm ribbon widths in the first-principles calculation become 11.4 and 4.75 meV, respectively. Thus, the ballistic electron thermal conductance per unit width of intrinsic graphene ribbons is thought to be much smaller than that of a graphene sheet by opening of the energy gap with narrowing the ribbon width and it approaches that of a graphene sheet at 100 K above $W_z=80$ nm and $W_a=50$ nm for zigzag ribbons and armcahir ribbons, respectively, due to reduction of the edge effect.

Third, we discuss about the relation between the ballistic electronic thermal conductance κ_{el} and the ballistic electronic conductance S for gated graphene ribbons. In the diffusive electronic transport of metal, it is well known that the Wiedemann-Franz law is satisfied between the electronic conductivity σ and the thermal conductivity κ of electrons.[24]

$$\frac{\kappa}{\sigma T}=L, \tag{5}$$

where L is called as the Lorentz number and it takes a constant value of $L_0=\frac{1}{3}\pi^2(\frac{k_B}{q})^2$.[24] If we evaluate the ballistic electronic conductance S of a gated graphene ribbon by assuming a small chemical-potential difference between two parallel gates, S is given by

$$S = \sum_m \frac{2q^2}{h} \int_{v_m(k)>0} dx_m \frac{\exp(x_m)}{[\exp(x_m)+1]^2}. \quad (6)$$

Here, $x_m=[\varepsilon_m(k)-\mu]/k_BT$ and the transmission coefficient is assumed to be unity. In low temperatures, S can be calculated as $S=2q^2/h$, $S=6q^2/h$, $S=10q^2/h$, and so on as the Fermi level increases, in the tight-binding model. This means that the Wiedemann-Franz law is satisfied with the same Lorentz number L_0 as the classical diffusive transport for metallic-gated graphene ribbons at low temperatures.

Next, we will discuss about the effects of assumed approximation on the numerical results. We adopted a simple tight-binding model to calculate the electronic band structure of graphene ribbons. It is a good approximation for both carbon nanotubes and a graphene sheet.[1] As mentioned above and in the first Sec. I, however, the ground state for zigzag ribbons with the sub-ten-nm width becomes antiferromagnetic with the up- and down-spin densities localized at the opposite edges.[14,21,23] A small energy gap opens at the Fermi energy in the band structure for each spin, contrary to the metallic nature in the tight-binding model. The bottom of the conduction band is located inside the Brillouin zone but the energy dispersion is very small between the bottom and the Brillouin-zone edge, keeping the nature of the flat band in the tight-binding model. The similar situation holds also for the top of the valence band, although the energy dispersion near the Brillouin-zone edge is larger than that of the conduction band. The calculated energy gaps in eV can be fit by $E_g=9.33/(W_z+15)$ with a width of W_z in angstroms below 7 nm.[14] For example, this relation gives $E_g=41$ meV at $W_z=21$ nm ($N_z=101$). However, the energy difference between the antiferromagnetic ground state and the ferrimagnetic excited state with the majority spin density localized at both edges is very small and the energy difference decreases with increasing ribbon width.[14] In the ferrimagnetic excited state, both the majority and the minority spin have the similar metallic band structure as that obtained by the tight-binding model, although a part of the flat band is occupied for the majority spin but unoccupied for the minority spin.[23] The ballistic thermal conductance is not sensitive to the detailed dispersion relation and the ferrimagnetic state gives the similar behavior as the ballistic thermal conductance calculated in the tight-binding approximation. We think that the tight-binding model can give the qualitative results for zigzag ribbons of $N_z>100$ in a temperature range of $T>100$ K. As for the armchair ribbons, on the other hand, the ground state for the metallic armcahir ribbons in the tight-binding model changes to semiconducting caused by both the edge relaxation and the quantum-confinement effect and a small energy gap opens at the Fermi energy.[14,22] The energy gap in eV decreases as $E_g=0.648/(p+1)$, where $N_a=3p+2$.[14] For example, E_g becomes 9.7 meV at $N_a=200$ ($W_a=25$ nm). Thus, we expect that the tight-binding model can give the qualitative results for armchair ribbons of $N_a>200$ in a temperature range of $T>100$ K. As for intrinsic graphene ribbons, they become semiconductors and the electron contribution to the normalized ballistic thermal conductance vanishes in low temperatures. The opening of the energy gap changes the quantized values of the normalized ballistic thermal conductance at $T=1$ K for gated graphene ribbons in Figs. 5 and 6 to $0,4,2,6,10\ldots$, for zigzag ribbons and to $0,2,6,10,\ldots$, for armcahir ribbons. The appearance of the plateau at 4 for zigzag ribbons is attributed to the small energy dispersion near the conduction-band edge.

With respect to scattering effect, we assumed the ballistic transport with the transmission coefficient of unity. This means our numerical results give the upper limit for the thermal conductance. As mentioned in the first Sec. I, the edge disorder is considered as the main scattering mechanism for graphene ribbons.[5] The localized character of the wave function at the flat band is maximum at $k=\pi/a_z$ for zigzag ribbons and decreases as the wave vector k decreases. The contribution to the thermal current arises from the region of positive group velocity, $v_m(k)>0$, and hence the contribution of the flat band is not included. This means that the thermal current is carried by the bulklike state and hence the edge disorder becomes not so sensitive for zigzag ribbons. Indeed, this insensitivity to irregular edges is shown for zigzag ribbons.[10] Scattering by irregular edges is the dominant scattering mechanism for narrow armchair ribbons.[10] However, the edge scattering mean-free path is proportional to the ribbon width[5] and hence a large mean-free path is expected for wide ribbons.

Finally, we mention scattering effect by electron-electron Coulomb interaction. In one-dimensional system, the Coulomb interactions cause strong perturbation on electrons near the Fermi level. The resulting system is predicted to be distictly different from the Fermi liquid and is called as the Luttinger liquid. In the Luttinger liquid, the forward scattering by the long-range part of the electron-electron interaction is renormalized. Recently, Zarea and Sandler showed for undoped metallic armchair ribbons that charge band gap opens in the Luttinger liquid state,[25] similar to the result in first-principles calculation.[14] The gap in the Luttinger liquid is caused by forward scattering by electron-electron interaction and the gap is reduced by both doping and increase in the ribbon width. The gap opening and the anomalous transport properties in the Luttinger liquid state were predicted for undoped metallic armchair carbon nanotubes.[26] The peculiar tunneling behavior into the Luttinger liquid was confirmed experimentally by measurements of the conductance of bundles of single-walled carbon nanotubes.[27] The gap opening is a serious issue in a one-dimensional system since it means that the Fermi liquid state does not become stable with respect to electron-electron interaction. However, the single-particle Fermi liquid picture describes many experimental results in nanotubes.[1] We expect the same situation for graphene ribbons with width above 20 nm.

In summary, we investigate the ballistic thermal conductance of electrons in gated graphene ribbons and clarify both the temperature and the Fermi-level dependences. In the intrinsic graphene ribbons, the normalized thermal conductance by the quantum conductance, κ_0, increases monotonically with temperature. In the gated graphene ribbons, the normalized thermal conductance of electrons increases steplikely as the Fermi level increases but the temperature dependence of the normalized thermal conductance exhibits nonmonotonic behavior. The value of a step height changes from $4\kappa_0$ to $2\kappa_0$ with increasing temperature. The ballistic electron thermal conductance per unit width of graphene ribbons is smaller than those of corresponding single-walled nanotubes and a graphene sheet. It approaches that of a graphene sheet at 100 K above the ribbon width of about 80 and 50 nm for zigzag ribbons and armchair ribbons, respectively, due to reduction of the edge effect.

ACKNOWLEDGMENT

We acknowledge T. Yamamoto for stimulating our interests on the ballistic thermal conductance of graphene ribbons. This was a trigger for this study.

*junj@ee.uec.ac.jp; http://www.natori.ee.uec.ac.jp/junj/
†natori@ee.uec.ac.jp

[1] R. Saito, G. Dresselhaus, and M. S. Dresselhaus, *Physical Properties of Carbon Nanotubes* (Imperial College, London, 1998).
[2] J. Hone, M. Whitney, C. Piskoti, and A. Zettl, Phys. Rev. B **59**, R2514 (1999).
[3] T. Yamamoto, S. Watanabe, and K. Watanabe, Phys. Rev. Lett. **92**, 075502 (2004).
[4] X. Li, X. Wang, L. Zhang, S. Lee, and H. Dai, Science **319**, 1229 (2008).
[5] X. Wang, Y. Ouyang, X. Li, H. Wang, J. Guo, and H. Dai, Phys. Rev. Lett. **100**, 206803 (2008).
[6] L. Jiao, L. Zhang, X. Wang, G. Diankov, and H. Dai, Nature (London) **458**, 877 (2009).
[7] D. V. Kosynkin, A. L. Higginbotham, A. Sinitskii, J. R. Lomeda, A. Dimiev, B. K. Price, and J. M. Tour, Nature (London) **458**, 872 (2009).
[8] J. Fernandez-Rossier, J. J. Palacios, and L. Brey, Phys. Rev. B **75**, 205441 (2007).
[9] F. Munoz-Rojas, J. Fernandez-Rossier, L. Brey, and J. J. Palacios, Phys. Rev. B **77**, 045301 (2008).
[10] D. A. Areshkin, D. Gunlycke, and C. T. White, Nano Lett. **7**, 204 (2007).
[11] M. Fujita, K. Wakabayashi, K. Nakada, and K. Kusakabe, J. Phys. Soc. Jpn. **65**, 1920 (1996).
[12] K. Nakada, M. Fujita, G. Dresselhaus, and M. S. Dresselhaus, Phys. Rev. B **54**, 17954 (1996).
[13] M. Y. Han, B. Ozyilmaz, Y. Zhang, and P. Kim, Phys. Rev. Lett. **98**, 206805 (2007).
[14] Y. W. Son, M. L. Cohen, and S. G. Louie, Phys. Rev. Lett. **97**, 216803 (2006).
[15] K. Saito, J. Nakamura, and A. Natori, Phys. Rev. B **76**, 115409 (2007).
[16] A. A. Balandin, S. Ghosh, W. Bao, I. Calizo, D. Teweldebrhan, F. Miao, and C. N. Lau, Nano Lett. **8**, 902 (2008).
[17] N. Mingo and D. A. Broido, Phys. Rev. Lett. **95**, 096105 (2005).
[18] T. Yamamoto, K. Watanabe, and K. Mii, Phys. Rev. B **70**, 245402 (2004).
[19] Y. Miyamoto, K. Nakada, and M. Fujita, Phys. Rev. B **59**, 9858 (1999).
[20] T. Kawai, Y. Miyamoto, O. Sugino, and Y. Koga, Phys. Rev. B **62**, R16349 (2000).
[21] S. Okada and A. Oshiyama, Phys. Rev. Lett. **87**, 146803 (2001).
[22] S. Okada, Phys. Rev. B **77**, 041408(R) (2008).
[23] J. Nakamura, T. Nitta, and A. Natori, Phys. Rev. B **72**, 205429 (2005).
[24] J. M. Ziman, *Electrons and Phonons* (Oxford University Press, Oxford, 1963).
[25] M. Zarea and N. Sandler, Phys. Rev. Lett. **99**, 256804 (2007).
[26] C. Kane, L. Balents, and M. P. A. Fisher, Phys. Rev. Lett. **79**, 5086 (1997).
[27] M. Bockrath, D. H. Cobden, J. Lu, A. G. Rinzler, R. E. Smalley, L. Balents, and P. L. McEuen, Nature (London) **397**, 598 (1999).